Technische Universität Dresden • Faculty of Mathematics

Derivation and study of a non-confluent model for deformable cells

Master's thesis

to obtain the second degree

Master of Science
(*M.Sc.*)

written by

Tim Vogel

(born on June 9, 2002 in Finsterwalde)

Day of submission: November 28, 2025

Supervised by Jun.-Prof. Dr. Markus Schmidtchen
(Institute of Scientific Computing)

Contents

1 TODOs **5**

2 Density computations **6**
2.1 1d needles example 9
2.2 DF model mean field PDE 14

3 Outlook **20**
3.1 Computation of $\nabla_{\vec{v}_j} \cdot \nabla_{\vec{v}_j} A_2(C)$ 20
3.2 Computation of $\nabla_{\vec{v}_j} \cdot \nabla_{\vec{v}_j} I_2(C)$ 24

Nomenclature

abbreviation	description
PDE	A partial differential equation is an equation that contains unknown multivariable functions and their partial derivatives.
SDE	A stochastic differential equation is a differential equation in which one or more of the terms is a stochastic process, resulting in a solution that is also a stochastic process.
DF model	The discrete form model is a vertex cell model that is defined by a list of all wall points.

Mathematical conventions

symbol	description
$\vec{v}$	Superscript arrows denote multidimensional variables
$\frac{\partial f}{\partial v}$	Partial derivative of a scalar function f with respect to a one dimensional variable v
$\nabla_{\vec{v}} f$	Gradient $\nabla_{\vec{v}} f = (\frac{\partial f}{\partial v_1}, \ldots, \frac{\partial f}{\partial v_n})^T$, where f is a scalar function and $\vec{v} = (v_1, \ldots, v_n)^T$ is a multidimensional variable
$\nabla_{\vec{v}} \cdot F$	Divergence $\nabla_{\vec{v}} \cdot F = \frac{\partial F_1}{\partial v_1} + \ldots + \frac{\partial F_n}{\partial v_n}$, where $F = (F_1, \ldots, F_m)^T$ is a vector valued function
$D_{\vec{v}} F$	Jacobian matrix $D_{\vec{v}} F = \begin{pmatrix} \frac{\partial F_1}{\partial v_1} \cdots \frac{\partial F_1}{\partial v_n} \\ \vdots \\ \frac{\partial F_m}{\partial v_1} \cdots \frac{\partial F_m}{\partial v_n} \end{pmatrix}$,
Δf	Laplacian of a scalar function f
$2e-3$	Scientific notation for $2 \times 10^{-3} = 0.002$
$\mathrm{d}\vec{B}_i(t)$	Two dimensional Brownian motion applied to cell i at time t in SDEs
I_d	Identity matrix in $\mathbb{R}^{d \times d}$
$\mathbb{R}_+$	Positive real numbers including 0, i.e. $[0, \infty)$
$\mathbb{N}$	Natural numbers excluding 0
$\mathbb{N}_0$	Natural numbers including 0
$N_C \in \mathbb{N}$	Number of cells in a model
$N_V \in \mathbb{N}$	Number of vertices of each cell in a model
$C^i = (\vec{v}_1^i, \ldots, \vec{v}_{N_V}^i)$	DF cell $1 \leqslant i \leqslant N_C$
$\vec{v}_j^i = (v_j^{i,x}, v_j^{i,y})^T \in \mathbb{R}^2$	Vertex $1 \leqslant j \leqslant N_V$ of DF cell $1 \leqslant i \leqslant N_C$
$P(t; \vec{x}_1, \ldots, \vec{x}_{N_C})$	Joint probability density function
$\rho(t; \vec{x})$, $\rho^{N_C}(t; \vec{x})$	First marginal function
$\bar{\rho}(t; \vec{x})$	Density in the mean field limit

1 TODOs

Density comps

- write in sentences
- implement corrections from 25.11.2025
- use pde d rho / dt = - div(rho grad E) for shape preserving forces, mind scaling factor
- think about mean field pde with interaction

Outlook

- gather input
- structurise
- add bridges to chapters
- formulate in sentences

general things

- ———————————————
- look up max thesis strucure
- problem: e.g. **Overall** is larger than

  Bounce overlap force

- reference chat
- check punctation and spaces in equations
- print a version for proof reading
- ———————————————
- add left(, right) where it is necessary
- control indices
- check dash -
- add references to introduction papers to all chapters
- be consistent in naming of DF model
- do a spell check to only use UK english
- inserrt correct gif links
- ———————————————

2 Density computations

In the previous chapter, we employed Monte Carlo simulations to validate the microscopic cell model and to illustrate the qualitative behaviour emerging from the underlying gradient flow dynamics. While such simulations provide valuable empirical insight, they do not yet reveal the macroscopic, continuum level structure of the system.

In this chapter, we therefore develop a systematic framework to pass from individual cell dynamics to a description in terms of probability measures and densities. We introduce the empirical measure associated with large ensembles of simulated cells, explain its convergence to the first marginal of the N_C cell system, and analyse the subsequent mean-field limit as $N_C \to \infty$.

This leads naturally to a deterministic transport equation for the limiting cell density, which provides a mathematically transparent interpretation of the collective dynamics. We illustrate this approach with an explicit low dimensional needle cell example. Afterwards, we compute the mean field PDEs for our DF model with sorely the area, edge or interior angle force applied, respectively. Unfortunately, we did not manage to do the same for our interaction term in this thesis, as there was not enough time. For our point particle monte carlo simulations, we can define the empirical measure

$$\begin{aligned} \mu_t^{(N_C,N_S)} : \mathcal{B}(\mathbb{R}^2) &\longrightarrow [0,1], \\ A \longmapsto \mu_t^{(N_C,N_S)}(A) &= \frac{1}{N_C N_S} \sum_{i=1}^{N_C} \sum_{s=1}^{N_S} \delta_{\vec{x}_i^{(s)}(t)}(A), \end{aligned}$$

where N_C is again the number of cells in each simulation, N_S denotes the number of simulations in the Monte Carlo simulation and $\vec{x}_i^{(s)}(t) \in \Omega \subset \mathbb{R}^2$ is the location of point particle $1 \leqslant i \leqslant N_C$ in simulation $1 \leqslant s \leqslant N_S$ and at time $t \in [0,T]$. $\mathcal{B}(\mathbb{R}^2)$ is the Borel sigma-algebra on $\mathbb{R}^2$ and $\delta_{\vec{x}_i(t)}$ denotes the Dirac measure:

$$\begin{aligned} \delta_{\vec{x}_i(t)} : \mathcal{B}(\mathbb{R}^2) &\longrightarrow \{0,1\}, \\ A \longmapsto \delta_{\vec{x}_i(t)}(A) &= \begin{cases} 1 & \text{if } \vec{x}_i(t) \in A, \\ 0 & \text{if } \vec{x}_i(t) \notin A. \end{cases} \end{aligned}$$

For any test function $\phi \in C_c^\infty(\mathbb{R}^2)$, the Dirac measure satisfies

$$\int_{\mathbb{R}^2} \phi(x) \mathrm{d}\delta_{\vec{x}_i(t)}(x) = \phi(\vec{x}_i(t)).$$

For a set $A \in \mathcal{B}(\mathbb{R}^2)$, the quantity $\mu_t^{(N_C,N_S)}(A)$ denotes the relative proportion of the N_C particles that lie in A at time t, averaged over all N_S simulations.

The heatmaps in Chapter **??** are obtained by evaluating this empirical measure on a family of subsets $\{A_{ij}\}_{i,j=1}^{N_H}$, where N_H^2 is the number of sub squares into which we partition the domain $\Omega = [-0.5, 0.5]^2$. Each subsquare A_{ij} has side length $\frac{1}{N_H}$, and increasing N_H yields an increasingly fine spatial resolution of Ω.

If, in addition, we let $N_S \to \infty$, then by the Central Limit Theorem the empirical heatmaps converge to their expectation, which coincides with the first marginal

distribution of the system, since the simulations are independent and identically distributed. In our computations we used 10 000 simulations to ensure a reliable numerical approximation of this first marginal.

There is also a further limit to consider: the mean field limit. Here, we let the number of cells $N_C \to \infty$. In the mean field limit, we can study the transition from the microscopic model view, that uses a finite number of cells, $N_C < \infty$, to a macroscopic model view where we consider the whole system's density without individual cells.
Figure 1 illustrates how empirical particle distributions converge towards their underlying mean field density as the number of particles increases. The first three panels depict empirical measures obtained from samples of size $N_C \in \{20, 200, 20\,000\}$, drawn independently from the same Gaussian distribution $\mathcal{N}_2((0,0), 0.09^2 I_2)$. To visualise these empirical measures, the domain $\Omega = [-0.5, 0.5]^2$ is partitioned into 50×50 sub squares, on which the empirical measure

$$\mu^{N_C}(A) = \frac{1}{N_C} \sum_{i=1}^{N_C} \delta_{\vec{x}_i}(A)$$

is evaluated and displayed as a heatmap.
As the particle number grows, the empirical distribution becomes progressively smoother and more faithful to the true underlying density. For small N_C, random fluctuations dominate the visual appearance, while for larger N_C these fluctuations average out, and the heatmap increasingly resembles the continuous Gaussian density shown in the fourth panel.

For the following discussion, we assume that the first marginal distributions of the DF model converge to a mean field density, that is,

$$\rho^{N_C} \xrightarrow{N_C \to \infty} \bar{\rho}.$$

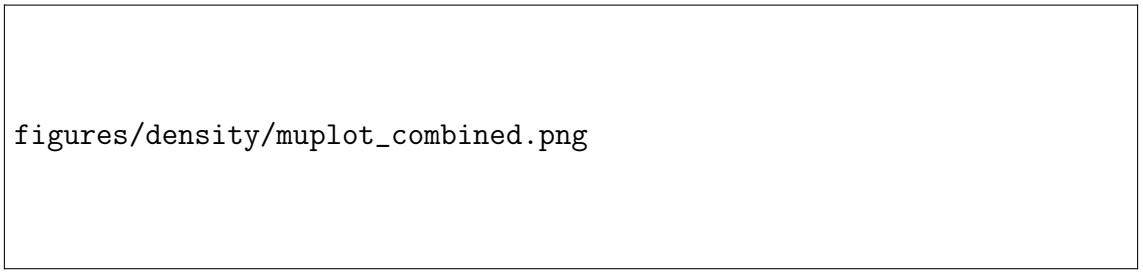

Figure 1: Empirical measures for increasing particle numbers $N_C \in \{20, 200, 20\,000\}$, compared with the limiting density $\mathcal{N}_2((0,0), 0.09^2 \cdot I_2)$ shown in the fourth panel. Particles are sampled i.i.d. from the same distribution, and the empirical measure μ^{N_C} is visualised on a 50×50 grid of sub squares. As N_C increases, the empirical heatmaps become smoother and converge to the Gaussian density, demonstrating the transition towards the mean field limit. A consistent colour scale allows direct comparison across all subplots.

In the preceding chapters, we wrote ρ for the first marginal, as the mean field limit was not under consideration. To emphasise the dependence on the number of cells N_C, we adopt the notation ρ^{N_C} throughout this chapter.
A rigorous analysis establishing this convergence remains an interesting direction for future work.

Next, we will show how the PDE for the mean field density temporal evolution can be computed generally for a point particle model, if the particle dynamic is given by the gradient flow of a given energy. For N_C point particles $\vec{x}_i(t) \in \mathbb{R}^2$, we use a cell wise energy

$$\begin{aligned} E : \mathbb{R}^2 &\longrightarrow \mathbb{R}, \\ \vec{x} &\longmapsto E(\vec{x}). \end{aligned}$$

We define the dynamic of a particle $\vec{x}_i$ via

$$\frac{\mathrm{d}\vec{x}_i(t)}{\mathrm{d}t} = -\nabla E(\vec{x}_i(t)) \in \mathbb{R}^2, \quad 1 \leqslant i \leqslant N_C.$$

We consider the empirical measure

$$\mu_t^{N_C}(A) = \tfrac{1}{N_C} \sum_{i=1}^{N_C} \delta_{\vec{x}_i(t)}(A)$$

Let $\phi \in C_c^\infty(\mathbb{R}^2, \mathbb{R})$ be a test function with gradient field $\nabla\phi : \mathbb{R}^2 \to \mathbb{R}^2$.
We assume that $\mu_t^{N_C}$ has density $\rho_t^{N_C}$ ($\mathrm{d}\mu_t^{N_C} = \rho_t^{N_C}(x)\mathrm{d}x$) and we have convergence

$$\rho_t^{N_C} \xrightarrow{N_C \to \infty} \bar{\rho}_t.$$

First, we consider

$$\begin{aligned} \frac{\mathrm{d}}{\mathrm{d}t} \int \phi(x)\, \mathrm{d}\mu_t^{N_C} &= \frac{\mathrm{d}}{\mathrm{d}t} \int \phi(x)\, \rho_t^{N_C}(x)\, \mathrm{d}x \\ &\xrightarrow{N_C \to \infty} \frac{\mathrm{d}}{\mathrm{d}t} \int \phi(x)\, \bar{\rho}_t(x)\, \mathrm{d}x \\ &= \int \phi(x)\, \frac{\partial}{\partial t} \left[\bar{\rho}_t(x)\right]\, \mathrm{d}x, \end{aligned} \tag{1}$$

using first the density $\rho_t^{N_C}$ of $\mu_t^{N_C}$ and then convergence $\rho_t^{N_C} \xrightarrow{N_C \to \infty} \bar{\rho}_t$.

Then, we use the definition of the empirical measure to obtain

$$
\begin{aligned}
\frac{\mathrm{d}}{\mathrm{d}t}\int \phi(x)\,\mathrm{d}\mu_t^{N_C} &= \frac{\mathrm{d}}{\mathrm{d}t}\left[\frac{1}{N_C}\sum_{i=1}^{N_C}\phi(\vec{x}_i^{(s)}(t))\right] \\
&= -\frac{1}{N_C}\sum_{i=1}^{N_C}\nabla\phi(\vec{x}_i^{(s)}(t))\cdot\nabla E(\vec{x}_i^{(s)}(t)) \\
&= -\int \nabla\phi(x)\cdot\nabla E(x)\,\mathrm{d}\mu_t^{N_C} \\
&= -\int \nabla\phi(x)\cdot\nabla E(x)\,\rho_t^{N_C}(x)\,\mathrm{d}x \\
&\xrightarrow{N_C\to\infty} -\int \nabla\phi(x)\cdot\nabla E(x)\,\bar{\rho}_t(x)\,\mathrm{d}x \\
&= \int \phi(x)\nabla\cdot(\bar{\rho}_t(x)\nabla E(x))\,\mathrm{d}x.
\end{aligned} \tag{2}
$$

We consider the difference from Equations (1) and (2) for $N_C \to \infty$

$$
\begin{aligned}
0 &= \int \phi(x)\,\frac{\partial}{\partial t}\left[\bar{\rho}_t(x)\right]\,\mathrm{d}x - \int \phi(x)\nabla\cdot(\bar{\rho}_t(x)\nabla E(x))\,\mathrm{d}x \\
&= \int \phi(x)\left(\frac{\partial}{\partial t}\left[\bar{\rho}_t(x)\right] - \nabla\cdot(\bar{\rho}_t(x)\nabla E(x))\right)\,\mathrm{d}x.
\end{aligned}
$$

As this holds true for any $\phi \in C_c^\infty(\mathbb{R}^2,\mathbb{R})$, we obtain the mean field PDE

$$
\frac{\partial\bar{\rho}_t(x)}{\partial t} - \nabla\cdot(\bar{\rho}_t(x)\nabla E(x)) = 0. \tag{3}
$$

For a force function $F(C) = -\nabla_C E(C)$, the we get the formulation

$$
\frac{\partial\bar{\rho}_t(x)}{\partial t} + \nabla\cdot(\bar{\rho}_t(x)F(x)) = 0. \tag{4}
$$

2.1 1d needles example

In order to demonstrate how the preceding computations can be applied in practice, we begin with a lower dimensional example. In this setting, each cell consists of two vertices situated in one spatial dimension,

$$
C = \{v_1, v_2\}, \quad v_1, v_2 \in \mathbb{R}
$$

where we assume $v_1 \neq v_2$ and that their ordering remains fixed throughout the simulation. This ensures that cells do not attain negative length.
Our dynamic naturally fulfils this condition, as we use the cell wise energy

$$
E(C) = \tfrac{1}{2}\left||v_1 - v_2| - E_d\right|^2,
$$

where E_d is the desired edge length of each cell. This energy lets each needle cell to recover a length of E_d.

Applying gradient flow dynamics yields

$$\begin{aligned}\frac{\mathrm{d}v_1}{\mathrm{d}t} &= -\nabla_{v_1} E(C)\\ &= -\nabla_{v_1} \tfrac{1}{2}||v_1 - v_2| - E_d|^2\\ &= -(|v_1 - v_2| - E_d)\nabla_{v_1}|v_1 - v_2|\\ &= -sgn(v_1 - v_2)(|v_1 - v_2| - E_d),\end{aligned}$$

and

$$\frac{\mathrm{d}v_2}{\mathrm{d}t} = sgn(v_1 - v_2)(|v_1 - v_2| - E_d).$$

The resulting cell dynamics take the compact form

$$\frac{\partial C}{\partial t} = -\nabla_C E(C) = F(C) = \underbrace{sgn(v_1 - v_2)(|v_1 - v_2| - E_d)}_{=\alpha} \begin{pmatrix} -1 \\ 1 \end{pmatrix}.$$

For the subsequent derivation we require the computations

$$\begin{aligned}\nabla_{v_1} \cdot \alpha &= \nabla_{v_1} \cdot (sgn(v_1 - v_2)(|v_1 - v_2| - E_d))\\ &= (\nabla_{v_1} \cdot sgn(v_1 - v_2))(|v_1 - v_2| - E_d) + sgn(v_1 - v_2)(\nabla_{v_1} \cdot (|v_1 - v_2| - E_d))\\ &= 0 + sgn(v_1 - v_2)(\nabla_{v_1} \cdot (|v_1 - v_2|))\\ &= sgn(v_1 - v_2)sgn(v_1 - v_2)\\ &= 1,\end{aligned}$$

and

$$\begin{aligned}\nabla_{v_2} \cdot \alpha &= \nabla_{v_2} \cdot (sgn(v_1 - v_2)(|v_1 - v_2| - E_d))\\ &= (\nabla_{v_2} \cdot sgn(v_1 - v_2))(|v_1 - v_2| - E_d) + sgn(v_1 - v_2)(\nabla_{v_2} \cdot (|v_1 - v_2| - E_d))\\ &= 0 + sgn(v_1 - v_2)(\nabla_{v_2} \cdot (|v_1 - v_2|))\\ &= sgn(v_1 - v_2)(-sgn(v_1 - v_2))\\ &= -1,\end{aligned}$$

With these identities at hand, we compute the divergence

$$\begin{aligned}\nabla_C \cdot (\bar{\rho}F) &= \nabla_{v_1} \cdot (\bar{\rho}F_1) + \nabla_{v_2} \cdot (\bar{\rho}F_2)\\ &= (\nabla_{v_1} \cdot \bar{\rho})F_1 + \bar{\rho}(\nabla_{v_1} \cdot F_1) + (\nabla_{v_2} \cdot \bar{\rho})F_2 + \bar{\rho}(\nabla_{v_2} \cdot F_2)\\ &= -(\nabla_{v_1} \cdot \bar{\rho})\alpha - \bar{\rho}(\nabla_{v_1} \cdot \alpha) + (\nabla_{v_2} \cdot \bar{\rho})\alpha + \bar{\rho}(\nabla_{v_2} \cdot \alpha)\\ &= -(\nabla_{v_1} \cdot \bar{\rho})\alpha - \bar{\rho} + (\nabla_{v_2} \cdot \bar{\rho})\alpha - \bar{\rho}\\ &= -2\bar{\rho} + \alpha(-\nabla_{v_1} \cdot \bar{\rho} + \nabla_{v_2} \cdot \bar{\rho})\end{aligned}$$

where $F = (F_1, F_2)^T$.
Consequently, in the mean field limit $N_C \to \infty$, the density $\bar{\rho}$ satisfies

$$\frac{\partial \bar{\rho}}{\partial t} + 2\bar{\rho} - \alpha(-\nabla_{v_1} \cdot \bar{\rho} + \nabla_{v_2} \cdot \bar{\rho}) = 0,$$

according to Equation (5).
To illustrate this model, we present two corresponding simulations. First, we consider a finite system of $N_C = 400$ needle cells. Each cell is initialised according to

$$C_i = (v_1^i, v_2^i) \sim \mathcal{N}_2((0.5, 0.5)^T, 0.09^2 \cdot I_2), \quad 1 \leqslant i \leqslant 400.$$

We then evolve the system under the dynamics

$$\frac{\partial C}{\partial t} = F(C) = sgn(v_1 - v_2)(|v_1 - v_2| - E_d)(-1, 1)^T,$$

using a desired edge length of $E_d = 0.2$. The resulting ODE system is integrated with an explicit Euler method using a time step of $\Delta t = 10^{-3}$ over the interval $[0, 1]$, giving 100 time steps.
Figure 2 visualises the evolution of the one dimensional needle cell system. Each cell is represented by a blue point in the (v_1, v_2) plane, where the horizontal axis corresponds to the position of the first vertex and the vertical axis to that of the second vertex. Such a representation is only possible in this lower-dimensional setting, since the full vertex configuration of a cell can be embedded in $\mathbb{R}^2$.
At initial time, the $N_C = 400$ cells are sampled from $\mathcal{N}_2((0.5, 0.5), 0.09^2 \cdot I_2)$. As time progresses, the dynamics drive each cell towards its desired edge length $E_d = 0.2$. In the scatter plot, this manifests as a gradual migration of points towards the two diagonal lines defined by $|v_1 - v_2| = 0.2$, corresponding to cells whose vertex separation has achieved the prescribed value. By the final time, all cells lie precisely on these two diagonals, confirming that the system converges to a configuration in which every cell has relaxed to the target length.

Subsequently, we examine the associated mean field dynamics. We choose an initial condition given by $\mathcal{N}_2((0.5, 0.5)^T, 0.09^2 \cdot I_2)$ on the domain $\Omega = [0.0, 1.0]^2$ and evolve it using the PDE

$$\frac{\partial \bar{\rho}}{\partial t} = \nabla_{v_1} \cdot (-\bar{\rho}\alpha) + \nabla_{v_2} \cdot (\bar{\rho}\alpha),$$

which arises from the earlier derivation of the density evolution equation. The

discretisation is given by

$$
\begin{aligned}
\Omega &\longrightarrow \{A_{ij}\}_{i,j=1}^{500} \text{ sub squares,} \\
\bar{\rho} &\longrightarrow \bar{\rho}_{ij}^{k} \text{ density value on } A_{ij} \text{ at time step } k \in \mathbb{N}, \\
\partial_t \bar{\rho} &\longrightarrow \frac{\bar{\rho}_{ij}^{k+1} - \bar{\rho}_{ij}^{k}}{\Delta t}, \\
\alpha &\longrightarrow \alpha_{ij}^{k} \text{ value on } A_{ij} \text{ at time step } k \in \mathbb{N}, \\
\nabla_{v_1} \cdot (-\bar{\rho}\alpha) &\longrightarrow \frac{-\bar{\rho}_{i,j+1}^{k}\alpha_{i,j+1}^{k} + \bar{\rho}_{i,j-1}^{k}\alpha_{i,j-1}^{k}}{2\Delta x}, \\
\nabla_{v_2} \cdot (\bar{\rho}\alpha) &\longrightarrow \frac{\bar{\rho}_{i+1,j}^{k}\alpha_{i+1,j}^{k} - \bar{\rho}_{i-1,j}^{k}\alpha_{i-1,j}^{k}}{2\Delta x},
\end{aligned}
$$

with grid spacing $\Delta x = \frac{1}{500}$.

Figure 2: Scatter plots showing the evolution of $N_C = 400$ one dimensional needle cells at times $t \in \{0.0, 0.2, \ldots, 1.0\}$. Each blue point represents a single cell, with the horizontal axis indicating the location of the first vertex v_1 and the vertical axis the location of the second vertex v_2. The initial conditions are drawn from $\mathcal{N}_2((0.5, 0.5), 0.09^2 \cdot I_2)$. The dynamics aim to achieve a desired edge length of $E_d = 0.2$, corresponding to the two diagonal lines defined by $|v_1 - v_2| = 0.2$.

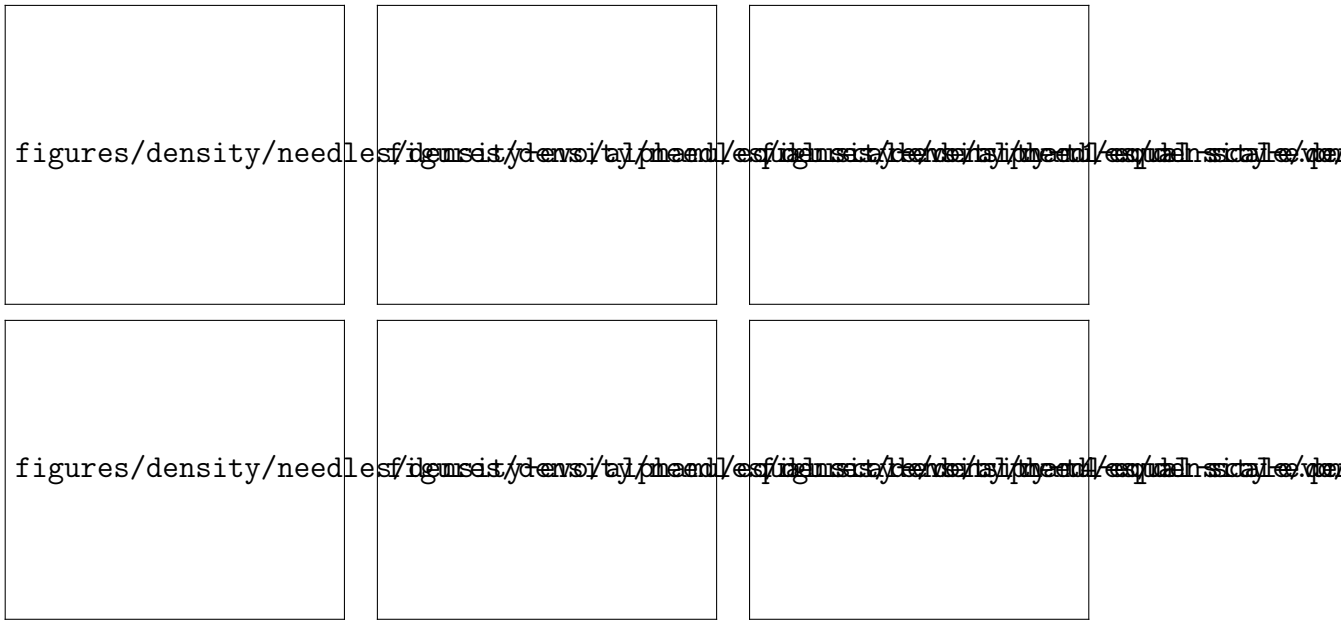

Figure 3: Evolution of the mean field density starting from the initial distribution $\mathcal{N}_2((0.5, 0.5), 0.09^2 \cdot I_2)$ on the domain $[0, 1]^2$. The PDE dynamics transport the density towards the two diagonal lines defined by $|v_1 - v_2| = 0.2$, along which the mass becomes concentrated over time. The plots display the density at successive time instances and include small oscillations between the diagonals arising from the central-difference discretisation; these could be removed through an upwind treatment of the spatial gradients.

Figure 3 illustrates the evolution of the cell density in the mean field limit. The initial distribution is given by $\mathcal{N}_2((0.5, 0.5), 0.09^2 \cdot I_2)$ on the domain $[0, 1]^2$, forming a concentrated region in the centre of the domain. Under the action of the mean field PDE, the density is gradually transported towards the two diagonal lines characterised by $|v_1 - v_2| = 0.2$, mirroring the behaviour observed in the finite-particle simulation from Figure 2. As time evolves, the solution develops sharp ridges along these diagonals, and by the final time almost all mass is concentrated on there, indicating convergence towards the desired edge length in the continuum description. During the evolution, small oscillations appear in the region between the two diagonals. These artefacts are purely numerical and originate from the central difference discretisation used for the spatial derivatives. They can be removed by employing an upwind scheme, which would provide the correct directional bias in the discretisation of the fluxes and thereby suppress non-physical oscillations.
Both simulations exhibit exclusion effects that closely resemble the behaviour observed in the earlier hard disc model shown in Figure **??**. In the hard disc example, the diagonal region of the domain was inaccessible because any placement of the second disc in that area would necessarily lead to overlap with the first disc. This exclusion was enforced explicitly: overlap was prohibited both by the initial configuration and by the dynamics, which strictly prevented discs from entering the forbidden region.
The geometric volume exclusion in the hard disc system corresponds to the desired state constraint in the needle model: whereas discs must avoid overlaps, needles are

driven toward configurations in which their length equals E_d, and both mechanisms create analogous forbidden regions in the state space. The needle model does not impose such exclusions a priori. Initially, needle cell configurations with lengths unequal to E_d are allowed. Nevertheless, the dynamics, driven by the energy term

$$E(C) = \tfrac{1}{2}||v_1 - v_2| - E_d|^2,$$

naturally steer the system toward states where the needle length matches E_d. As the evolution proceeds, the density gradually depletes along the diagonal region of the (v_1, v_2) space, reproducing the same 'forbidden' diagonal line that appeared in the hard-disc case.
Thus, while the hard disc model exhibits a hard exclusion (geometric non-overlap), the needle system develops a soft exclusion: the dynamics energetically penalize undesirable configurations until the system self organises into a feasible state.

2.2 DF model mean field PDE

- bridge from needle example to mean field DF PDE Now, we want to apply the computation for PDE (3) on our DF model. Therefore, we adapt our empirical measure. In the DF model, we model cells as polygons with $N_V \in \mathbb{N}$ vertices. Thus, we need to use δ_{C_i} that uses high dimensional subsets $A \subset \mathbb{R}^{2N_V}$, i.e.

$$\begin{aligned} \mu_t^{(N_C,N_V)} &: \mathcal{B}(\mathbb{R}^{2N_V}) \longrightarrow [0,1], \\ A \longmapsto \mu_t^{(N_C,N_V)}(A) &= \frac{1}{N_C}\sum_{i=1}^{N_C} \delta_{C_i(t)}(A), \end{aligned}$$

where $C_i(t) = (\vec{v}_1^{\,i}, \ldots, \vec{v}_{N_V}^{\,i})$ is cell i at time t.
We use a cell wise energy

$$E : \mathbb{R}^{2N_V} \to \mathbb{R},$$

with gradient

$$\nabla E : \mathbb{R}^{2N_V} \to \mathbb{R}^{2N_V}.$$

Later on, we want to insert the three shape preserving energies, i.e. the area, edge and interior angle energy, that all have the above attributes. We can derive the mean field PDE for this setup as follows. Let $\phi \in C_c^\infty(\mathbb{R}^{2N_V}, \mathbb{R})$ be a test function on the higher dimensional space $\mathbb{R}^{2N_V}$. We assume that the empirical measure $\mu_t^{(N_C,N_V)}$ has density $\rho_t^{(N_C,N_V)}$ that converges to the mean field density $\bar{\rho}_t^{N_V}$, as $N_C \to \infty$. Similarly to the calculation at the beginning of this chapter, we observe

$$\begin{aligned} \frac{\mathrm{d}}{\mathrm{d}t}\int \phi(C)\,\mathrm{d}\mu_t^{(N_C,N_V)} &= \frac{\mathrm{d}}{\mathrm{d}t}\int \phi(C)\,\rho_t^{(N_C,N_V)}(C)\,\mathrm{d}C \\ &\xrightarrow{N_C\to\infty} \frac{\mathrm{d}}{\mathrm{d}t}\int \phi(C)\,\bar{\rho}_t^{N_V}(C)\,\mathrm{d}C \\ &= \int \phi(C)\,\frac{\partial}{\partial t}\left[\bar{\rho}_t^{N_V}(C)\right]\,\mathrm{d}C, \end{aligned}$$

and

$$\begin{aligned}
\frac{\mathrm{d}}{\mathrm{d}t}\int \phi(C)\,\mathrm{d}\mu_t^{(N_C,N_V)} &= \frac{\mathrm{d}}{\mathrm{d}t}\left[\frac{1}{N_C}\sum_{i=1}^{N_C}\phi(C_i(t))\right] \\
&= -\frac{1}{N_C}\sum_{i=1}^{N_C}\nabla\phi(C_i(t))\cdot\nabla E(C_i(t)) \\
&= -\int \nabla\phi(C)\cdot\nabla E(C)\,\mathrm{d}\mu_t^{(N_C,N_V)} \\
&= -\int \nabla\phi(C)\cdot\nabla E(C)\,\rho_t^{(N_C,N_V)}(C)\,\mathrm{d}C \\
&\xrightarrow{N_C\to\infty} -\int \nabla\phi(C)\cdot\nabla E(C)\,\bar{\rho}_t^{N_V}(C)\,\mathrm{d}C \\
&= \int \phi(C)\nabla\cdot(\bar{\rho}_t^{N_V}(C)\nabla E(C))\,\mathrm{d}C.
\end{aligned}$$

We can conclude, with the same derivation as before, that

$$\frac{\partial\bar{\rho}_t^{N_V}(C)}{\partial t} - \nabla\cdot(\bar{\rho}_t^{N_V}(C)\nabla E(C)) = 0. \tag{5}$$

Now, we want to consider our energies individually, before we take a look at a combined system. We define the vector of all vertex coordinates of cell C as

$$V_C = (v_1^x, v_1^y, \ldots, v_{N_V}^x, v_{N_V}^y)^T \in \mathbb{R}^{2N_V}.$$

Area energy

First, we consider pure scaled area energy, i.e.

$$E_A(C) = \alpha_A A_2(C) = \frac{\alpha_A}{2}|A_C - A_d|^2,$$

with $A_2(C)$ defined at Equation (**??**) with $k = 2$.
This energy has the gradient

$$\nabla_C E_A(C) = \begin{pmatrix} \nabla_{\vec{v}_1} \\ \vdots \\ \nabla_{\vec{v}_{N_V}} \end{pmatrix} E_A(C),$$

with

$$\begin{aligned}
\nabla_{\vec{v}_j} E_A(C) &= \alpha_A \nabla_{\vec{v}_j} A_2(C) \\
&= \frac{\alpha_A}{2}(A_C - A_d)\begin{pmatrix} v_{j+1}^y - v_{j-1}^y \\ v_{j-1}^x - v_{j+1}^x \end{pmatrix},
\end{aligned}$$

where we used

$$\nabla_{\vec{v}_j} A_2(C) = \frac{1}{2}(A_C - A_d) \begin{pmatrix} v^y_{j+1} - v^y_{j-1} \\ v^x_{j-1} - v^x_{j+1} \end{pmatrix},$$

from Equation (**??**).
We conclude the matrix $M_A \in \mathbb{R}^{2N_V \times 2N_V}$ as

$$M_A = \begin{pmatrix} 0 & 0 & \boxed{\begin{matrix} 0 & 1 \\ -1 & 0 \end{matrix}} & 0 & 0 & \cdots & 0 & 0 & \boxed{\begin{matrix} 0 & -1 \\ 1 & 0 \end{matrix}} \\ 0 & 0 & & 0 & 0 & & 0 & 0 & \\ \boxed{\begin{matrix} 0 & -1 \\ 1 & 0 \end{matrix}} & & 0 & 0 & \boxed{\begin{matrix} 0 & 1 \\ -1 & 0 \end{matrix}} & 0 & 0 & \cdots & 0 & 0 \\ & & 0 & 0 & & 0 & 0 & & 0 & 0 \\ & & & \ddots & & & \ddots & & & \\ 0 & 0 & & \cdots & 0 & 0 & \boxed{\begin{matrix} 0 & -1 \\ 1 & 0 \end{matrix}} & 0 & 0 & \boxed{\begin{matrix} 0 & 1 \\ -1 & 0 \end{matrix}} \\ 0 & 0 & & & 0 & 0 & & 0 & 0 & \\ \boxed{\begin{matrix} 0 & 1 \\ -1 & 0 \end{matrix}} & & 0 & 0 & & 0 & 0 & \boxed{\begin{matrix} 0 & -1 \\ 1 & 0 \end{matrix}} & 0 & 0 \\ & & 0 & 0 & \cdots & 0 & 0 & & 0 & 0 \end{pmatrix},$$

such that, we can write down the cell wise gradient as

$$\nabla_C E_A(C) = \frac{\alpha_A}{2}(A_C - A_d) \begin{pmatrix} v^y_2 - v^y_{N_V} \\ v^x_{N_V} - v^x_2 \\ \vdots \\ v^y_1 - v^y_{N_V - 1} \\ v^x_{N_V - 1} - v^x_1 \end{pmatrix} = \frac{\alpha_A}{2}(A_C - A_d) M_A V_C \tag{6}$$

Edge energy

Now, we want to consider the exclusive scaled edge energy, i.e.

$$E_E(C) = \alpha_E E_2(C) = \frac{\alpha_E}{2} \sum_{j=1}^{N_V} |E^j_C - E^j_d|^2,$$

with actual edge length $E^j_C = \|\vec{v}_j - \vec{v}_{j+1}\|_2$ and desired length E^j_d at edge j. We took $E_2(C)$ from Equation (**??**) with $k = 2$. In this case we can compute the gradient as

$$\nabla_C E_E(C) = \begin{pmatrix} \nabla_{\vec{v}_1} \\ \vdots \\ \nabla_{\vec{v}_{N_V}} \end{pmatrix} E_E(C),$$

with

$$\begin{aligned}\nabla_{\vec{v}_j} E_E(C) &= \alpha_E \nabla_{\vec{v}_j} E_2(C) \\ &= \alpha_E \left(\frac{E_C^{j-1} - E_d^{j-1}}{E_C^{j-1}} \begin{pmatrix} v_j^x - v_{j-1}^x \\ v_j^y - v_{j-1}^y \end{pmatrix} + \frac{E_C^j - E_d^j}{E_C^j} \begin{pmatrix} v_j^x - v_{j+1}^x \\ v_j^y - v_{j+1}^y \end{pmatrix} \right),\end{aligned}$$

where we used

$$\nabla_{\vec{v}_j} E_2(C) = \frac{E_C^{j-1} - E_d^{j-1}}{E_C^{j-1}} \begin{pmatrix} v_j^x - v_{j-1}^x \\ v_j^y - v_{j-1}^y \end{pmatrix} + \frac{E_C^j - E_d^j}{E_C^j} \begin{pmatrix} v_j^x - v_{j+1}^x \\ v_j^y - v_{j+1}^y \end{pmatrix},$$

from Equation (**??**).
If we define matrices for the prefactors: $D_E, D_{E-} \in \mathbb{R}^{2N_V \times 2N_V}$ as

$$D_E = \operatorname{diag}\left(\frac{E_C^1 - E_d^1}{E_C^1}, \frac{E_C^1 - E_d^1}{E_C^1}, \ldots, \frac{E_C^{N_V} - E_d^{N_V}}{E_C^{N_V}}, \frac{E_C^{N_V} - E_d^{N_V}}{E_C^{N_V}} \right),$$

and

$$D_{E-} = \operatorname{diag}\left(\tfrac{E_C^{N_V} - E_d^{N_V}}{E_C^{N_V}}, \tfrac{E_C^{N_V} - E_d^{N_V}}{E_C^{N_V}}, \tfrac{E_C^1 - E_d^1}{E_C^1}, \tfrac{E_C^1 - E_d^1}{E_C^1}, \ldots, \tfrac{E_C^{N_V-1} - E_d^{N_V-1}}{E_C^{N_V-1}} \right).$$

And rewrite the following parts as

$$M_E = \begin{pmatrix} \boxed{\begin{matrix} 1 & 0 \\ 0 & 1 \end{matrix}} & \boxed{\begin{matrix} -1 & 0 \\ 0 & -1 \end{matrix}} & \begin{matrix} 0 & 0 \\ 0 & 0 \end{matrix} & \cdots & & \begin{matrix} 0 & 0 \\ 0 & 0 \end{matrix} \\ & \ddots & \ddots & & & \\ & & & & & \\ \begin{matrix} 0 & 0 \\ 0 & 0 \end{matrix} & & & \begin{matrix} 0 & 0 \\ 0 & 0 \end{matrix} & \boxed{\begin{matrix} 1 & 0 \\ 0 & 1 \end{matrix}} & \boxed{\begin{matrix} -1 & 0 \\ 0 & -1 \end{matrix}} \\ \boxed{\begin{matrix} -1 & 0 \\ 0 & -1 \end{matrix}} & \begin{matrix} 0 & 0 \\ 0 & 0 \end{matrix} & \cdots & & \begin{matrix} 0 & 0 \\ 0 & 0 \end{matrix} & \boxed{\begin{matrix} 1 & 0 \\ 0 & 1 \end{matrix}} \end{pmatrix} \in \mathbb{R}^{2N_V \times 2N_V},$$

and

$$M_{E-} = \begin{pmatrix} \boxed{\begin{matrix} 1 & 0 \\ 0 & 1 \end{matrix}} & \begin{matrix} 0 & 0 \\ 0 & 0 \end{matrix} & \cdots & & \begin{matrix} 0 & 0 \\ 0 & 0 \end{matrix} & \boxed{\begin{matrix} -1 & 0 \\ 0 & -1 \end{matrix}} \\ \boxed{\begin{matrix} -1 & 0 \\ 0 & -1 \end{matrix}} & \boxed{\begin{matrix} 1 & 0 \\ 0 & 1 \end{matrix}} & \begin{matrix} 0 & 0 \\ 0 & 0 \end{matrix} & \cdots & & \begin{matrix} 0 & 0 \\ 0 & 0 \end{matrix} \\ & & \ddots & \ddots & & \\ & & & & & \\ \begin{matrix} 0 & 0 \\ 0 & 0 \end{matrix} & & & \begin{matrix} 0 & 0 \\ 0 & 0 \end{matrix} & \boxed{\begin{matrix} -1 & 0 \\ 0 & -1 \end{matrix}} & \boxed{\begin{matrix} 1 & 0 \\ 0 & 1 \end{matrix}} \end{pmatrix} \in \mathbb{R}^{2N_V \times 2N_V}.$$

We can conclude a cell wise edge energy gradient as

$$\nabla_C E_E(C) = \alpha_E \left(D_{E-} M_{E-} + D_E M_E\right) V_C. \tag{7}$$

Interior angle energy

Next, we consider a system with pure scaled interior angle energy, i.e.

$$E_I(C) = \alpha_I I_2(C) = \frac{\alpha_I}{2} \sum_{j=1}^{N_V} |I_C^j - I_d^j|^2$$

where we used

$$I_2(C) = \sum_{j=1}^{N_V} \frac{1}{2} |I_C^j - I_d^j|^2,$$

from Equation (**??**) with $k = 2$.
In Chapter **??**, we already computed the first derivative as

$$\begin{aligned}
\nabla_{\vec{v}_j} I_2(C) = (I_C^{j-1} - I_d^{j-1}) &\left(-\frac{1}{(E_C^j)^2} \begin{pmatrix} v_{j-1}^y - v_j^y \\ v_j^x - v_{j-1}^x \end{pmatrix} \right) \\
&+ (I_C^j - I_d^j) \left(\frac{1}{(E_C^j)^2} \begin{pmatrix} v_{j-1}^y - v_j^y \\ v_j^x - v_{j-1}^x \end{pmatrix} - \frac{1}{(E_C^{j+1})^2} \begin{pmatrix} v_{j+1}^y - v_j^y \\ v_j^x - v_{j+1}^x \end{pmatrix} \right) \\
&+ (I_C^{j+1} - I_d^{j+1}) \left(\frac{1}{(E_C^{j+1})^2} \begin{pmatrix} v_{j+1}^y - v_j^y \\ v_j^x - v_{j+1}^x \end{pmatrix} \right),
\end{aligned}$$

in Equation (**??**).
We define the matrices $D_I, D_{I-}, D_{I+} \in \mathbb{R}^{2N_V \times 2N_V}$ as

$$\begin{aligned}
D_I &= \operatorname{diag}\big(I_C^1 - I_d^1, I_C^1 - I_d^1, I_C^2 - I_d^2, I_C^2 - I_d^2, \ldots, I_C^{N_V} - I_d^{N_V}, I_C^{N_V} - I_d^{N_V}\big), \\
D_{I-} &= \operatorname{diag}\big(I_C^{N_V} - I_d^{N_V}, I_C^{N_V} - I_d^{N_V}, I_C^1 - I_d^1, I_C^1 - I_d^1, \ldots, I_C^{N_V-1} - I_d^{N_V-1}, I_C^{N_V-1} - I_d^{N_V-1}\big), \\
D_{I+} &= \operatorname{diag}\big(I_C^2 - I_d^2, I_C^2 - I_d^2, \ldots, I_C^{N_V} - I_d^{N_V}, I_C^{N_V} - I_d^{N_V}, I_C^1 - I_d^1, I_C^1 - I_d^1\big).
\end{aligned}$$

The terms of form $\frac{1}{(E_C^j)^2}$ and $\frac{1}{(E_C^{j+1})^2}$ are summerised in $B_I, B_{I+} \in \mathbb{R}^{2N_V \times 2N_V}$ as,

$$\begin{aligned}
B_I &= \operatorname{diag}\big((E_C^1)^{-2}, (E_C^1)^{-2}, \ldots, (E_C^{N_V})^{-2}, (E_C^{N_V})^{-2}\big), \\
B_{I+} &= \operatorname{diag}\big((E_C^2)^{-2}, (E_C^2)^{-2}, \ldots, (E_C^{N_V})^{-2}, (E_C^{N_V})^{-2}, (E_C^1)^{-2}, (E_C^1)^{-2}\big).
\end{aligned}$$

Finally, we put together missing vertex terms with matrices $M_{I-}, M_{I+} \in \mathbb{R}^{2N_V \times 2N_V}$ as

$$M_{I-} = \begin{pmatrix} \boxed{\begin{matrix} 0 & -1 \\ 1 & 0 \end{matrix}} & \begin{matrix} 0 & 0 \\ 0 & 0 \end{matrix} & \cdots & & \begin{matrix} 0 & 0 \\ 0 & 0 \end{matrix} & \boxed{\begin{matrix} 0 & 1 \\ -1 & 0 \end{matrix}} \\ \boxed{\begin{matrix} 0 & 1 \\ -1 & 0 \end{matrix}} & \boxed{\begin{matrix} 0 & -1 \\ 1 & 0 \end{matrix}} & \begin{matrix} 0 & 0 \\ 0 & 0 \end{matrix} & \cdots & & \begin{matrix} 0 & 0 \\ 0 & 0 \end{matrix} \\ & & \ddots & \ddots & & \\ \begin{matrix} 0 & 0 \\ 0 & 0 \end{matrix} & \cdots & & \begin{matrix} 0 & 0 \\ 0 & 0 \end{matrix} & \boxed{\begin{matrix} 0 & 1 \\ -1 & 0 \end{matrix}} & \boxed{\begin{matrix} 0 & -1 \\ 1 & 0 \end{matrix}} \end{pmatrix},$$

$$M_{I+} = \begin{pmatrix} \boxed{\begin{matrix} 0 & -1 \\ 1 & 0 \end{matrix}} & \boxed{\begin{matrix} 0 & 1 \\ -1 & 0 \end{matrix}} & \begin{matrix} 0 & 0 \\ 0 & 0 \end{matrix} & \cdots & & \begin{matrix} 0 & 0 \\ 0 & 0 \end{matrix} \\ & & \ddots & \ddots & & \\ \begin{matrix} 0 & 0 \\ 0 & 0 \end{matrix} & \cdots & & \begin{matrix} 0 & 0 \\ 0 & 0 \end{matrix} & \boxed{\begin{matrix} 0 & -1 \\ 1 & 0 \end{matrix}} & \boxed{\begin{matrix} 0 & 1 \\ -1 & 0 \end{matrix}} \\ \boxed{\begin{matrix} 0 & 1 \\ -1 & 0 \end{matrix}} & \begin{matrix} 0 & 0 \\ 0 & 0 \end{matrix} & \cdots & & \begin{matrix} 0 & 0 \\ 0 & 0 \end{matrix} & \boxed{\begin{matrix} 0 & -1 \\ 1 & 0 \end{matrix}} \end{pmatrix}.$$

We can write down the cell wise interior angle gradient as

$$\nabla_C E_I(C) = \alpha_I \left(-D_{I-} B_I M_{I-} + D_I \left(B_I M_{I-} - B_{I+} M_{I+}\right) + D_{I+} B_{I+} M_{I+}\right) V_C. \tag{8}$$

Shape preserving energies

If we now consider a combination of the three shape preserving energies, i.e.

$$E_{\text{shape}}(C) = E_A(C) + E_E(C) + E_I(C),$$

we can use the linearity of the gradient to easily write down

$$\nabla_C E_{\text{shape}}(C) = \nabla_C E_A(C) + \nabla_C E_E(C) + \nabla_C E_I(C). \tag{9}$$

The three gradients are given in the Equations (6), (7) and (8).

3 Outlook

An interesting extension of the current model would involve assigning individual desired states to each cell, in contrast to the uniform desired state used throughout this study. This modification would naturally lead to cell-specific energies and corresponding forces, as both would depend on the unique desired configuration of each cell. Incorporating such heterogeneity could allow the model to capture more complex biological behaviors, such as differentiation, cell-type-specific migration, or adaptive responses to environmental cues. - incorporate external force f,
- curved surfaces - 3d - cell division - more parameter studies - use more vertices for more accurate shape and dynamics - limit $N_V \to \infty$ - overdamping - new shapes - Additionally, many vertex models incorporate rules that govern changes in connection among vertices, and therefore allow for changes in cell neighbor relationships. -¿ These approximations are suitable in the case of tightly packed cell sheets, where the intercellular space is negligible, and is based on experimental observations that cells in epithelial tissues are often arranged in polygonal or polyhedral structures (19) and can move around relative to other cells (20) - mention that doing the cross section plot with a finer spatial resolution shows oscillations that are numerical artifacts - mean field limit for our overlap forces - existence of mean field limit density

3.1 Computation of $\nabla_{\vec{v}_j} \cdot \nabla_{\vec{v}_j} A_2(C)$

Now, we consider pure area energy

$$A_2(C) = \frac{1}{2}|A_C - A_d|^2,$$

defined at Equation (**??**) with $k = 2$.
The area gradient is given by

$$\nabla_{\vec{v}_j} A_2(C) = \frac{1}{2}(A_C - A_d) \begin{pmatrix} v_{j+1}^y - v_{j-1}^y \\ v_{j-1}^x - v_{j+1}^x \end{pmatrix},$$

in Equation (**??**).

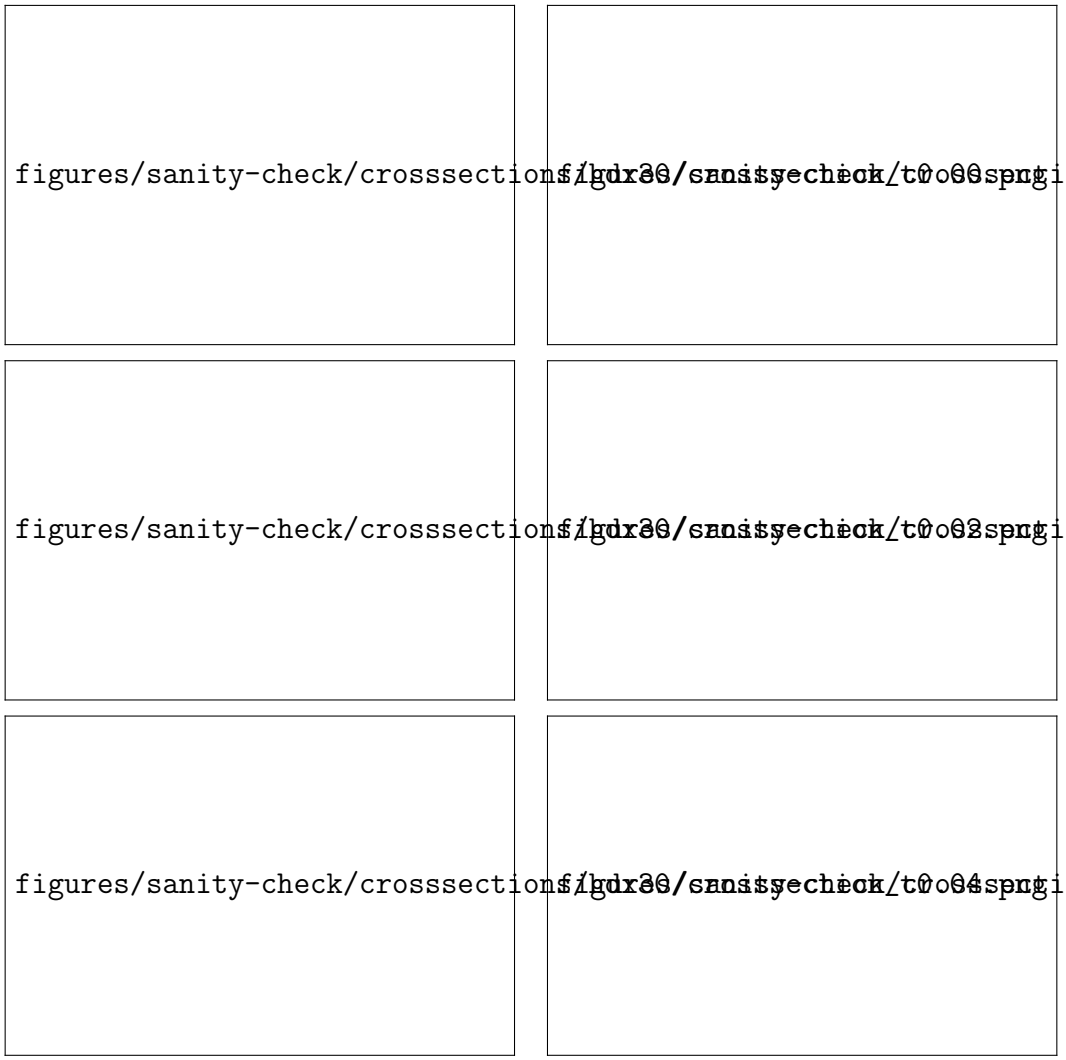

Figure 4

We compute the second derivative

$$\nabla_{\vec{v}_j} \cdot \nabla_{\vec{v}_j} A_2(C) = \nabla_{\vec{v}_j} \cdot \left[\frac{1}{2}(A_C - A_d) \begin{pmatrix} v^y_{j+1} - v^y_{j-1} \\ v^x_{j-1} - v^x_{j+1} \end{pmatrix} \right]$$

$$= \frac{1}{2} \left(\frac{\partial}{\partial v^x_j} \left[(A_C - A_d)(v^y_{j+1} - v^y_{j-1}) \right] + \frac{\partial}{\partial v^y_j} \left[(A_C - A_d)(v^x_{j-1} - v^x_{j+1}) \right] \right)$$

$$= \frac{1}{2} \left((v^y_{j+1} - v^y_{j-1}) \frac{\partial}{\partial v^x_j} \left[A_C \right] + (v^x_{j-1} - v^x_{j+1}) \frac{\partial}{\partial v^y_j} \left[A_C \right] \right)$$

$$= \frac{1}{2} \Bigg((v^y_{j+1} - v^y_{j-1}) \frac{\partial}{\partial v^x_j} \left[\frac{1}{2} \sum_{l=1}^{N} (v^x_l v^y_{l+1} - v^x_{l+1} v^y_l) \right] +$$
$$+ (v^x_{j-1} - v^x_{j+1}) \frac{\partial}{\partial v^y_j} \left[\frac{1}{2} \sum_{l=1}^{N} (v^x_l v^y_{l+1} - v^x_{l+1} v^y_l) \right] \Bigg)$$

$$= \frac{1}{2} \Bigg((v^y_{j+1} - v^y_{j-1}) \frac{1}{2} \frac{\partial}{\partial v^x_j} \left[(v^x_j v^y_{j+1} - v^x_{j+1} v^y_j) + (v^x_{j-1} v^y_j - v^x_j v^y_{j-1}) \right] +$$
$$+ (v^x_{j-1} - v^x_{j+1}) \frac{1}{2} \frac{\partial}{\partial v^y_j} \left[(v^x_j v^y_{j+1} - v^x_{j+1} v^y_j) + (v^x_{j-1} v^y_j - v^x_j v^y_{j-1}) \right] \Bigg)$$

Computation of $\nabla_{\vec{v}_j} \cdot \nabla_{\vec{v}_j} E_2(C)$

The gradient is given by

$$\nabla_{\vec{v}_j} E_2(C) = \frac{E_C^{j-1} - E_d^{j-1}}{E_C^{j-1}} \begin{pmatrix} v_j^x - v_{j-1}^x \\ v_j^y - v_{j-1}^y \end{pmatrix} + \frac{E_C^j - E_d^j}{E_C^j} \begin{pmatrix} v_j^x - v_{j+1}^x \\ v_j^y - v_{j+1}^y \end{pmatrix}.$$

For the following computation, we use the derivatives

$$\begin{aligned} \frac{\partial}{\partial v_j^x} E_C^{j-1} &= \frac{\partial}{\partial v_j^x} \|\vec{v}_{j-1} - \vec{v}_j\|_2 \\ &= \frac{\partial}{\partial v_j^x} \left[\left((v_{j-1}^x - v_j^x)^2 + (v_{j-1}^y - v_j^y)^2 \right)^{\frac{1}{2}} \right] \\ &= \frac{1}{2\|\vec{v}_{j-1} - \vec{v}_j\|_2} \frac{\partial}{\partial v_j^x} \left[(v_{j-1}^x - v_j^x)^2 + (v_{j-1}^y - v_j^y)^2 \right] \\ &= -\frac{v_{j-1}^x - v_j^x}{\|\vec{v}_{j-1} - \vec{v}_j\|_2} \\ &= \frac{v_j^x - v_{j-1}^x}{E_C^{j-1}}, \end{aligned}$$

and similarly

$$\frac{\partial}{\partial v_j^x} E_C^j = \frac{v_j^x - v_{j+1}^x}{E_C^j}, \quad \frac{\partial}{\partial v_j^y} E_C^{j-1} = \frac{v_j^y - v_{j-1}^y}{E_C^{j-1}}, \quad \frac{\partial}{\partial v_j^y} E_C^j = \frac{v_j^y - v_{j+1}^y}{E_C^j}.$$

We also need

$$\begin{aligned} \frac{\partial}{\partial v_j^x} \left[\frac{E_C^{j-1} - E_d^{j-1}}{E_C^{j-1}} \right] &= \frac{\partial}{\partial v_j^x} \left[1 - \frac{E_d^{j-1}}{E_C^{j-1}} \right] \\ &= -E_d^{j-1} \frac{\partial}{\partial v_j^x} \left[(E_C^{j-1})^{-1} \right] \\ &= -E_d^{j-1} (-(E_C^{j-1})^{-2}) \frac{\partial}{\partial v_j^x} \left[E_C^{j-1} \right] \\ &= \frac{E_d^{j-1}}{(E_C^{j-1})^2} \frac{v_j^x - v_{j-1}^x}{E_C^{j-1}} \\ &= \frac{E_d^{j-1}}{(E_C^{j-1})^3} (v_j^x - v_{j-1}^x), \end{aligned}$$

and, respectively

$$\frac{\partial}{\partial v_j^x} \left[\frac{E_C^j - E_d^j}{E_C^j} \right] = \frac{E_d^j}{(E_C^j)^3} (v_j^x - v_{j+1}^x), \quad \frac{\partial}{\partial v_j^y} \left[\frac{E_C^{j-1} - E_d^{j-1}}{E_C^{j-1}} \right] = \frac{E_d^{j-1}}{(E_C^{j-1})^3} (v_j^y - v_{j-1}^y),$$

$$\frac{\partial}{\partial v_j^y} \left[\frac{E_C^j - E_d^j}{E_C^j} \right] = \frac{E_d^j}{(E_C^j)^3} (v_j^y - v_{j+1}^y).$$

We continue with the computation of the second derivative of the first summand in the first derivative of the edge energy

$$
\begin{aligned}
\nabla_{\vec{v}_j} \cdot \left[\frac{E_C^{j-1} - E_d^{j-1}}{E_C^{j-1}} \begin{pmatrix} v_j^x - v_{j-1}^x \\ v_j^y - v_{j-1}^y \end{pmatrix} \right] &= \\
&= \frac{\partial}{\partial v_j^x} \left[\frac{E_C^{j-1} - E_d^{j-1}}{E_C^{j-1}} (v_j^x - v_{j-1}^x) \right] + \frac{\partial}{\partial v_j^y} \left[\frac{E_C^{j-1} - E_d^{j-1}}{E_C^{j-1}} (v_j^y - v_{j-1}^y) \right] \\
&= \frac{\partial}{\partial v_j^x} \left[\frac{E_C^{j-1} - E_d^{j-1}}{E_C^{j-1}} \right] (v_j^x - v_{j-1}^x) + \frac{E_C^{j-1} - E_d^{j-1}}{E_C^{j-1}} \frac{\partial}{\partial v_j^x} \left[(v_j^x - v_{j-1}^x) \right] \\
&\quad + \frac{\partial}{\partial v_j^y} \left[\frac{E_C^{j-1} - E_d^{j-1}}{E_C^{j-1}} \right] (v_j^y - v_{j-1}^y) + \frac{E_C^{j-1} - E_d^{j-1}}{E_C^{j-1}} \frac{\partial}{\partial v_j^y} \left[(v_j^y - v_{j-1}^y) \right] \\
&= \frac{E_d^{j-1}}{(E_C^{j-1})^3} (v_j^x - v_{j-1}^x)(v_j^x - v_{j-1}^x) + \frac{E_C^{j-1} - E_d^{j-1}}{E_C^{j-1}} \\
&\quad + \frac{E_d^{j-1}}{(E_C^{j-1})^3} (v_j^y - v_{j-1}^y)(v_j^y - v_{j-1}^y) + \frac{E_C^{j-1} - E_d^{j-1}}{E_C^{j-1}} \\
&= \frac{E_d^{j-1}}{(E_C^{j-1})^3} (\underbrace{(v_j^x - v_{j-1}^x)^2 + (v_j^y - v_{j-1}^y)^2}_{= (E_C^{j-1})^2}) + \frac{2(E_C^{j-1} - E_d^{j-1})}{E_C^{j-1}} \\
&= \frac{E_d^{j-1}}{E_C^{j-1}} + \frac{2(E_C^{j-1} - E_d^{j-1})}{E_C^{j-1}} \\
&= \frac{2E_C^{j-1} - E_d^{j-1}}{E_C^{j-1}} \\
&= 2 - \frac{E_d^{j-1}}{E_C^{j-1}}.
\end{aligned}
$$

The computation for the second summand is analogous and it yields

$$
\nabla_{\vec{v}_j} \cdot \left[\frac{E_C^{j} - E_d^{j}}{E_C^{j}} \begin{pmatrix} v_j^x - v_{j+1}^x \\ v_j^y - v_{j+1}^y \end{pmatrix} \right] = 2 - \frac{E_d^{j}}{E_C^{j}}.
$$

Overall, we get

$$
\nabla_{\vec{v}_j} \cdot \nabla_{\vec{v}_j} E_2(C) = 4 - \frac{E_d^{j-1}}{E_C^{j-1}} - \frac{E_d^{j}}{E_C^{j}}.
$$

With that result, we can finally compute the searched divergence

$$\begin{aligned}
\nabla_C \cdot (\bar{\rho}\, \nabla_C E_2(C)) &= \sum_{j=1}^{N_V} \nabla_{\vec{v}_j} \cdot (\bar{\rho}\, \nabla_{\vec{v}_j} E_2(C)) \\
&= \sum_{j=1}^{N_V} \left((\nabla_{\vec{v}_j} \cdot \bar{\rho}) \cdot \nabla_{\vec{v}_j} E_2(C) + \bar{\rho}\, (\nabla_{\vec{v}_j} \cdot \nabla_{\vec{v}_j} E_2(C)) \right) \\
&= \sum_{j=1}^{N_V} \left((\nabla_{\vec{v}_j} \cdot \bar{\rho}) \cdot \nabla_{\vec{v}_j} E_2(C) + \bar{\rho}\, (4 - \frac{E_d^{j-1}}{E_C^{j-1}} - \frac{E_d^j}{E_C^j}) \right) \\
&= \sum_{j=1}^{N_V} \left((\nabla_{\vec{v}_j} \cdot \bar{\rho}) \cdot \nabla_{\vec{v}_j} E_2(C) \right) + \bar{\rho}\, (4N_V - 2 \sum_{j=1}^{N_V} \frac{E_d^j}{E_C^j}),
\end{aligned}$$

because

$$\sum_{j=1}^{N_V} (4 - \frac{E_d^{j-1}}{E_C^{j-1}} - \frac{E_d^j}{E_C^j}) = 4N_V - 2 \sum_{j=1}^{N_V} \frac{E_d^j}{E_C^j},$$

as we still use circular indexing, e.g. $E_C^0 = E_C^{N_V}$.

3.2 Computation of $\nabla_{\vec{v}_j} \cdot \nabla_{\vec{v}_j} I_2(C)$

For the energy

$$I_2(C) = \sum_{j=1}^{N_V} \frac{1}{2} |I_C^j - I_d^j|^2,$$

from Equation (**??**) with $k = 2$, we are looking for the second derivative.
In Chapter **??**, we already computed the first derivative as

$$\begin{aligned}
\nabla_{\vec{v}_j} I_2(C) = &\underbrace{(I_C^{j-1} - I_d^{j-1}) \left(-\frac{1}{\|\vec{v}_j - \vec{v}_{j-1}\|_2^2} \begin{pmatrix} v_{j-1}^y - v_j^y \\ v_j^x - v_{j-1}^x \end{pmatrix} \right)}_{=\psi_1(C)} \\
&+ \underbrace{(I_C^j - I_d^j) \left(\frac{1}{\|\vec{v}_{j-1} - \vec{v}_j\|_2^2} \begin{pmatrix} v_{j-1}^y - v_j^y \\ v_j^x - v_{j-1}^x \end{pmatrix} - \frac{1}{\|\vec{v}_{j+1} - \vec{v}_j\|_2^2} \begin{pmatrix} v_{j+1}^y - v_j^y \\ v_j^x - v_{j+1}^x \end{pmatrix} \right)}_{=\psi_2(C)} \\
&+ \underbrace{(I_C^{j+1} - I_d^{j+1}) \left(\frac{1}{\|\vec{v}_j - \vec{v}_{j+1}\|_2^2} \begin{pmatrix} v_{j+1}^y - v_j^y \\ v_j^x - v_{j+1}^x \end{pmatrix} \right)}_{=\psi_3(C)},
\end{aligned}$$

in Equation (**??**).

TODO: check sims for ψ_1 and ψ_3

Computation of $\nabla_{\vec{v}_j} \cdot \psi_1$

From the proof of Proposition **??**, we use

$$\frac{\partial}{\partial v_j^x}\left[I_C^j - I_d^j\right] = \frac{v_{j-1}^y - v_j^y}{(E_C^{j-1})^2}, \quad \frac{\partial}{\partial v_j^y}\left[I_C^j - I_d^j\right] = \frac{v_j^x - v_{j-1}^x}{(E_C^{j-1})^2},$$
$$\Longrightarrow \nabla_{\vec{v}_j}\left[I_C^j - I_d^j\right] = \frac{1}{(E_C^{j-1})^2}\begin{pmatrix} v_{j-1}^y - v_j^y \\ v_j^x - v_{j-1}^x \end{pmatrix}.$$

We continue with

$$\begin{aligned}
\frac{\partial}{\partial v_j^x}\left[\frac{v_{j-1}^y - v_j^y}{(E_{j-1}^C)^2}\right] &= (v_{j-1}^y - v_j^y)\frac{\partial}{\partial v_j^x}\left[(E_C^{j-1})^{-2}\right] \\
&= (v_{j-1}^y - v_j^y)\left(-2(E_C^{j-1})^{-3}\frac{\partial}{\partial v_j^x}\left[E_{j-1}^C\right]\right) \\
&= (v_{j-1}^y - v_j^y)\left(-2(E_C^{j-1})^{-3}\frac{v_j^x - v_{j-1}^x}{E_C^{j-1}}\right) \\
&= (v_{j-1}^y - v_j^y)\left(-2(E_C^{j-1})^{-4}(v_j^x - v_{j-1}^x)\right) \\
&= -\frac{2}{(E_C^{j-1})^4}(v_j^x - v_{j-1}^x)(v_{j-1}^y - v_j^y),
\end{aligned}$$

where we used the derivative

$$\frac{\partial}{\partial v_j^x}\left[E_C^{j-1}\right] = \frac{v_j^x - v_{j-1}^x}{E_C^{j-1}},$$

computed in the previous Subsection **??**.
Similarly, we get

$$\frac{\partial}{\partial v_j^y}\left[\frac{v_j^x - v_{j-1}^x}{(E_{j-1}^C)^2}\right] = -\frac{2}{(E_C^{j-1})^4}(v_j^x - v_{j-1}^x)(v_{j-1}^y - v_j^y) = \frac{\partial}{\partial v_j^x}\left[\frac{v_{j-1}^y - v_j^y}{(E_{j-1}^C)^2}\right],$$
$$\Longrightarrow \nabla_{\vec{v}_j} \cdot \left[\frac{1}{(E_C^{j-1})^2}\begin{pmatrix} v_{j-1}^y - v_j^y \\ v_j^x - v_{j-1}^x \end{pmatrix}\right] = -\frac{4}{(E_C^{j-1})^4}(v_j^x - v_{j-1}^x)(v_{j-1}^y - v_j^y).$$

Thus, we can compute

$$\begin{aligned}
\nabla_{\vec{v}_j} \cdot \psi_1(C) &= \nabla_{\vec{v}_j} \cdot \left[(I_C^{j-1} - I_d^{j-1}) \left(-\frac{1}{(E_C^{j-1})^2} \begin{pmatrix} v_{j-1}^y - v_j^y \\ v_j^x - v_{j-1}^x \end{pmatrix} \right) \right] \\
&= \left(\nabla_{\vec{v}_j} \left[I_C^{j-1} - I_d^{j-1} \right] \right) \cdot \left(-\frac{1}{(E_C^{j-1})^2} \begin{pmatrix} v_{j-1}^y - v_j^y \\ v_j^x - v_{j-1}^x \end{pmatrix} \right) \\
&+ (I_C^{j-1} - I_d^{j-1}) \nabla_{\vec{v}_j} \cdot \left[-\frac{1}{(E_C^{j-1})^2} \begin{pmatrix} v_{j-1}^y - v_j^y \\ v_j^x - v_{j-1}^x \end{pmatrix} \right] \\
&= \left(\frac{1}{(E_C^{j-1})^2} \begin{pmatrix} v_{j-1}^y - v_j^y \\ v_j^x - v_{j-1}^x \end{pmatrix} \right) \cdot \left(-\frac{1}{(E_C^{j-1})^2} \begin{pmatrix} v_{j-1}^y - v_j^y \\ v_j^x - v_{j-1}^x \end{pmatrix} \right) \\
&+ (I_C^{j-1} - I_d^{j-1}) \left(\frac{4}{(E_C^{j-1})^4} (v_j^x - v_{j-1}^x)(v_{j-1}^y - v_j^y) \right) \\
&= -\frac{1}{(E_C^{j-1})^4} (\underbrace{(v_{j-1}^y - v_j^y)^2 + (v_j^x - v_{j-1}^x)^2}_{=(E_C^{j-1})^2}) \\
&+ (I_C^{j-1} - I_d^{j-1}) \left(\frac{4}{(E_C^{j-1})^4} (v_j^x - v_{j-1}^x)(v_{j-1}^y - v_j^y) \right) \\
&= -\frac{1}{(E_C^{j-1})^2} + \frac{4}{(E_C^{j-1})^4} (I_C^{j-1} - I_d^{j-1})(v_j^x - v_{j-1}^x)(v_{j-1}^y - v_j^y).
\end{aligned}$$

Computation of $\nabla_{\vec{v}_j} \cdot \psi_2$

In a similar fashion, we can also compute

$$\nabla_{\vec{v}_j} \cdot \psi_3(C) = -\frac{1}{(E_C^j)^2} - \frac{4}{(E_C^j)^4} (I_C^{j-1} - I_d^{j-1})(v_j^x - v_{j+1}^x)(v_{j+1}^y - v_j^y)$$

Computation of $\nabla_{\vec{v}_j} \cdot \psi_3$

We get the second derivative

$$\begin{aligned}
\nabla_{\vec{v}_j} \cdot \nabla_{\vec{v}_j} I_2(C) = &\frac{2}{E_{j-1}^2} \left[1 + 2(I_C^{j-1} - I_d^{j-1} + I_C^j - I_d^j)(v_j^x - v_{j-1}^x)(v_j^y - v_{j-1}^y) \right] \\
&+ \frac{2}{E_j^2} \left[1 - 2(I_C^j - I_d^j + I_C^{j+1} - I_d^{j+1})(v_j^x - v_{j+1}^x)(v_j^y - v_{j+1}^y) \right] \\
&- \frac{2}{E_{j-1}^2 E_j^2} \left[(v_j^x - v_{j-1}^x)(v_j^x - v_{j+1}^x) + (v_j^y - v_{j-1}^y)(v_j^y - v_{j+1}^y) \right].
\end{aligned}$$

Statement of authorship

I hereby declare that I have written this thesis (*Derivation and study of a non-confluent model for deformable cells*) under the supervision of Jun.-Prof. Dr. Markus Schmidtchen independently and have listed all used sources and aids. I am submitting this thesis for the first time as part of an examination. I understand that attempted deceit will result in the failing grade „not sufficient“ (5.0).

Tim Vogel

Dresden, November 28, 2025

Technische Universität Dresden

Matriculation Number: 4930487

References